REPORT DOCUMENTATION PAGE

Form Approved OMB NO. 0704-0188

1. REPORT DATE (DD-MM-YYYY)	2. REPORT TYPE	3. DATES COVERED (From - To)
30-03-2011	Final Report	10-Dec-2008 - 9-Dec-2009

4. TITLE AND SUBTITLE
Inverted Organic Photovoltaic Cells on Lightweight, and Flexible Metal Foil Substrates

5a. CONTRACT NUMBER
W911NF-09-1-0034

5b. GRANT NUMBER

5c. PROGRAM ELEMENT NUMBER
8G10AR

6. AUTHORS
Stephen R. Forrest

5d. PROJECT NUMBER

5e. TASK NUMBER

5f. WORK UNIT NUMBER

7. PERFORMING ORGANIZATION NAMES AND ADDRESSES
University of Michigan - Ann Arbor
Regents of the University of Michigan
3003 S. State St
Ann Arbor, MI 48109 -1274

8. PERFORMING ORGANIZATION REPORT NUMBER

9. SPONSORING/MONITORING AGENCY NAME(S) AND ADDRESS(ES)
U.S. Army Research Office
P.O. Box 12211
Research Triangle Park, NC 27709-2211

10. SPONSOR/MONITOR'S ACRONYM(S)
ARO

11. SPONSOR/MONITOR'S REPORT NUMBER(S)
55658-PH-DRP.1

12. DISTRIBUTION AVAILIBILITY STATEMENT
Approved for Public Release; Distribution Unlimited

13. SUPPLEMENTARY NOTES
The views, opinions and/or findings contained in this report are those of the author(s) and should not contrued as an official Department of the Army position, policy or decision, unless so designated by other documentation.

14. ABSTRACT
In this program, we demonstrated high-efficiency small-molecule photovoltaic cells based on subphthalocyanine (SubPc)/C60 planar heterojunctions with an inverted layer sequence compared with conventional organic cells. The top-illuminated inverted device achieves a power conversion efficiency of 2.4 ± 0.2%, or approximately 75% that of a conventional planar SubPc/C60 solar cell on indium-tin-oxide-coated glass (with a power efficiency of 3.3 ± 0.1%). The open-circuit voltage of the inverted devices, optimized by tailoring the work function of the layers

15. SUBJECT TERMS

16. SECURITY CLASSIFICATION OF:			17. LIMITATION OF ABSTRACT	15. NUMBER OF PAGES	19a. NAME OF RESPONSIBLE PERSON
a. REPORT	b. ABSTRACT	c. THIS PAGE			Stephen Forrest
UU	UU	UU	UU		19b. TELEPHONE NUMBER 734-647-1147

Report Title

Inverted Organic Photovoltaic Cells on Lightweight, and Flexible Metal Foil Substrates

ABSTRACT

In this program, we demonstrated high-efficiency small-molecule photovoltaic cells based on subphthalocyanine (SubPc)/C60 planar heterojunctions with an inverted layer sequence compared with conventional organic cells. The top-illuminated inverted device achieves a power conversion efficiency of 2.4 ± 0.2%, or approximately 75% that of a conventional planar SubPc/C60 solar cell on indium-tin-oxide-coated glass (with a power efficiency of 3.3 ± 0.1%). The open-circuit voltage of the inverted devices, optimized by tailoring the work function of the layers adjacent to the donor and acceptor, is comparable to the conventional cell. This work suggests that the inverted devices are promising for use on opaque and/or flexible surfaces.

List of papers submitted or published that acknowledge ARO support during this reporting period. List the papers, including journal references, in the following categories:

(a) Papers published in peer-reviewed journals (N/A for none)

Number of Papers published in peer-reviewed journals: 0.00

(b) Papers published in non-peer-reviewed journals or in conference proceedings (N/A for none)

Number of Papers published in non peer-reviewed journals: 0.00

(c) Presentations

Number of Presentations:

Non Peer-Reviewed Conference Proceeding publications (other than abstracts):

Number of Non Peer-Reviewed Conference Proceeding publications (other than abstracts):

Peer-Reviewed Conference Proceeding publications (other than abstracts):

Number of Peer-Reviewed Conference Proceeding publications (other than abstracts):

(d) Manuscripts

Number of Manuscripts:

Patents Submitted

Patents Awarded

Awards

Graduate Students

NAME	PERCENT_SUPPORTED

FTE Equivalent:
Total Number:

Names of Post Doctorates

NAME	PERCENT_SUPPORTED

FTE Equivalent:
Total Number:

Names of Faculty Supported

NAME	PERCENT_SUPPORTED

FTE Equivalent:
Total Number:

Names of Under Graduate students supported

NAME	PERCENT_SUPPORTED

FTE Equivalent:
Total Number:

Student Metrics

This section only applies to graduating undergraduates supported by this agreement in this reporting period

The number of undergraduates funded by this agreement who graduated during this period: .....
The number of undergraduates funded by this agreement who graduated during this period with a degree in science, mathematics, engineering, or technology fields:.....
The number of undergraduates funded by your agreement who graduated during this period and will continue to pursue a graduate or Ph.D. degree in science, mathematics, engineering, or technology fields:.....
Number of graduating undergraduates who achieved a 3.5 GPA to 4.0 (4.0 max scale): .....
Number of graduating undergraduates funded by a DoD funded Center of Excellence grant for Education, Research and Engineering: .....
The number of undergraduates funded by your agreement who graduated during this period and intend to work for the Department of Defense .....
The number of undergraduates funded by your agreement who graduated during this period and will receive scholarships or fellowships for further studies in science, mathematics, engineering or technology fields: .....

Names of Personnel receiving masters degrees

NAME

Total Number:

Names of personnel receiving PHDs

NAME
Total Number:

Names of other research staff

NAME	PERCENT SUPPORTED
FTE Equivalent:	
Total Number:	

Sub Contractors (DD882)

Inventions (DD882)

Scientific Progress

Technology Transfer

Inverted Organic Photovoltaic Cells on Lightweight, and Flexible Metal Foil Substrates

Stephen R. Forrest
Departments of EECS, Physics and Materials Science & Engineering
University of Michigan, Ann Arbor, MI 48109 stevefor@umich.edu

Abstract

In this program, we demonstrated high-efficiency small-molecule photovoltaic cells based on subphthalocyanine (SubPc)/C_{60} planar heterojunctions with an inverted layer sequence compared with conventional organic cells. The top-illuminated inverted device achieves a power conversion efficiency of 2.4 ± 0.2%, or approximately 75% that of a conventional planar SubPc/C_{60} solar cell on indium-tin-oxide-coated glass (with a power efficiency of 3.3 ± 0.1%). The open-circuit voltage of the inverted devices, optimized by tailoring the work function of the layers adjacent to the donor and acceptor, is comparable to the conventional cell. This work suggests that the inverted devices are promising for use on opaque and/or flexible surfaces.

Our task in this DARPA program was to demonstrate organic solar cells that have the potential for being mounted on flexible substrates such as metal foils. Conventional OPVs are deposited onto, and illuminated through a glass substrate coated with a transparent conductor, e.g. indium tin oxide (ITO). Top-illuminated devices that eliminate the need for a glass substrate are of interest because they can be deposited onto opaque, light-weight and possibly flexible materials allowing for use in cost-efficient architectures such as in roll-deployable solar cells, power-generating paints or other coatings, as is required by the DoD for mounting on tents and other flexible substrates.

In a conventional small-molecule OPV cell (with the structure: transparent substrate/ ITO anode/donor/acceptor/metal cathode), a buffer layer such as bathocuproine (BCP) is inserted between the acceptor and cathode to prevent exciton quenching[1]. Despite its high (relative to vacuum) lowest unoccupied molecular orbital (LUMO) energy, BCP provides efficient electron transport through defect states created when the metal cathode is deposited onto the organic; however, these states are largely absent for inverted organic-on-metal interfaces[2]. To address this issue, previous top-illuminated devices utilized a bottom metal anode and a transparent top cathode (thin metal[3-5] or ITO[6]) without changing the deposition sequence of the organic layers or the polarity of the electrodes. Although defect states at the cathode are present in such structures, the resulting solar cells have limited efficiency because the optical field distribution is not optimal relative to the position of the donor and acceptor layers. For example, the C_{60} acceptor absorbs short wavelength light between λ = 400 nm and 500 nm, and thus should be placed near the reflective metal cathode, while the phthalocyanine donor absorbs longer wavelengths, and hence should optimally be adjacent to the transparent anode. Note that “inverted” has also been used to describe bulk polymer cells where the carrier collection direction is changed upon

insertion of metal oxides such as TiO_2 or MoO_3[7,8]. It was found that the MoO_3 pins the open-circuit voltage (V_{OC}) by screening the effects of the top electrode[7].

In this work, we demonstrate a top-illuminated organic solar cell based on vacuum-deposited subphthalocyanine (SubPc) and C_{60}, with an inverted layer structure optimized for maximum absorption of the optical field. Efficient electron extraction is achieved by eliminating the BCP layer, thereby also eliminating the need for defect-induced injection into this material. A MoO_3 buffer layer is deposited between the donor and the sputtered ITO top electrode. In addition to preventing damage to the donor layer during ITO deposition, MoO_3 contributes to hole extraction and the suppression of electron leakage[9]. The effects of varying the MoO_3 layer thickness and cathode materials are also investigated.

To prepare both conventional and inverted devices shown schematically in Fig. 1, bare and ITO-coated glass substrates were cleaned by a standard solvent regimen followed by UV-ozone treatment[10]. Materials were deposited at a rate of 2 Å/s for metals, and 1 Å/s for purified organics and MoO_3 in a high-vacuum (base pressure $< 4 \times 10^{-7}$ Torr) thermal evaporation chamber. Prior to the deposition of the top contact, samples were transferred to a high purity N_2 ambient (< 1 ppm H_2O and O_2) where a shadow mask defining arrays of 1 mm-diameter circular openings was attached. The top ITO contact was sputter-deposited at a power of 40W (0.2 Å/s) and a pressure of 2 mTorr using Ar plasma[11]. All deposition rates and thicknesses were measured by quartz crystal monitors and checked by variable-angle spectroscopic ellipsometry. Device performance was measured in air using a semiconductor parameter analyzer in the dark and under illumination from a 150 W Xe lamp with AM1.5G filters using standard procedures[12]. Lamp intensity was varied with neutral density filters and measured by an NREL-calibrated Si photodiode. A transfer-matrix formalism was used to simulate the optical field and absorption,

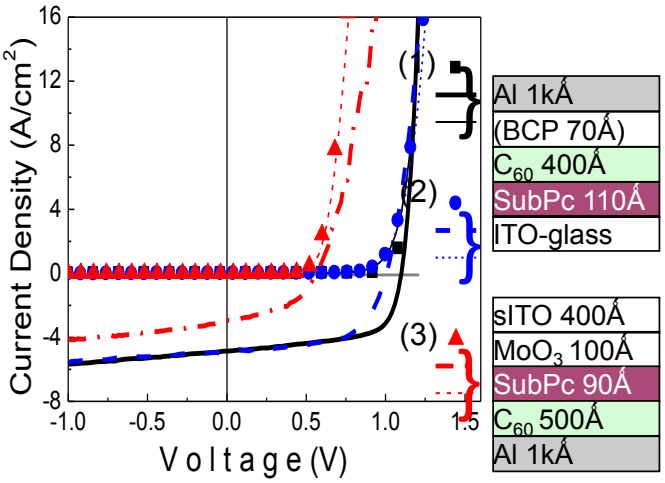

FIG. 1. (Color online) Current density *vs.* voltage characteristics of conventional and inverted solar cells with the structure (1) indium tin oxide (ITO)-coated glass/SubPc 110 Å/C_{60} 400 Å/BCP 70 Å/Al 1000 Å in the dark (squares) and under 1 sun, AM1.5G simulated illumination (solid line); (2) ITO-coated glass/SubPc 110 Å/C_{60} 400 Å/Al 1000 Å in the dark (circles) and under 1 sun, AM1.5G simulated illumination (dashed line); and (3) glass/Al 1000 Å/C_{60} 500 Å/SubPc 90 Å/MoO_3 100 Å/ITO 400 Å in the dark (triangles) and under 1 sun, AM1.5G simulated illumination (dash-dotted line). Fits according to the theory in text are indicated by the thin solid line, short dashed line and short dash-dotted line for devices (1), (2) and (3), respectively. The light is incident via ITO.

and to predict the short-circuit current (J_{SC}) of the devices[1]. The absorption spectra of the materials were measured using a Lambda 1050 UV/Vis/NIR spectrophotometer.

Previously, conventional planar small molecule OPVs lacking a BCP blocking-layer have exhibited greatly reduced efficiency[13,14]; however, we find that SubPc/C_{60} devices with Al cathodes can achieve similar performance without BCP, yet is sensitive to the C_{60} layer thickness. The comparable performance is achieved when C_{60} is thick enough to prevent the excitons generated within a diffusion length of the donor-acceptor (DA) interface from migrating to the metal-C_{60} interface where they quench, yet is not too thick to negatively impact performance by increasing resistance or placing the peak optical absorption far from the DA interface. Under simulated, 1 sun AM1.5G illumination, the device with BCP (Device 1, Fig. 1) showed a responsivity ($R = J_{SC}/P_0$, where P_0 is the incident light intensity) of 0.048 ± 0.001 A/W, a fill factor FF = 0.63 ± 0.01, and V_{OC} = 1.10 ± 0.02 V, leading to a power conversion efficiency of η_P = 3.3 ± 0.1%, while the device without BCP (Device 2, Fig. 1) achieved η_P = 3.0 ± 0.2%, with R = 0.049 ± 0.001 A/W, FF = 0.61 ± 0.03 and V_{OC} = 1.01 ± 0.02 V.

To prevent damage to the donor during ITO deposition, a MoO_3 buffer layer was inserted into the following inverted structure: glass/Al 1000 Å /C_{60} 500 Å /SubPc 90 Å/MoO_3 100 Å/ITO 400 Å (Device 3 in Fig. 1). This device showed η_P = 0.86 ± 0.08%, with R = 0.032 ± 0.002 A/W, FF = 0.48 ± 0.01 and V_{OC} = 0.56 ± 0.02 V under 1 sun, AM1.5G illumination. For the inverted device, the ideality factor n = 2.0 ± 0.1, series resistance R_{SA} = 4.9 ± 0.1 Ω·cm^2, and reverse saturation current density, J_S = (2 ± 1) × 10^{-5} mA/cm^2, were obtained by fitting the dark current-voltage (J_D-V) characteristics with the modified Shockley equation[15].

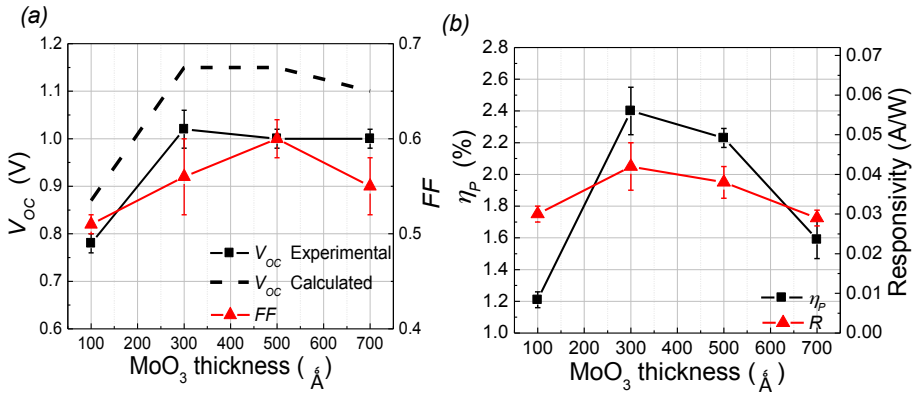

FIG. 2. (Color online) Device characteristics measured under simulated 1 sun, AM1.5G illumination for the structure: glass/Mg:Ag 1000 Å/C_{60} 500 Å/SubPc 90 Å/MoO_3 t Å/ITO 400 Å where t = 100, 300, 500, and 700. *(a)* Measured open-circuit voltage, V_{OC} (squares), calculated V_{OC} (dashed lines), and fill factor, FF (triangles) *vs.* MoO_3 thickness. *(b)* Power conversion efficiency, η_P (squares), and responsivity R (triangles) *vs.* MoO_3 thickness.

The low V_{OC} of the inverted device is attributed to the lower work function of sputtered ITO (4.03eV) as compared to commercially-deposited and UV-Ozone-treated ITO (4.7eV) used in the conventional cell[11]. This decreases the built-in electric field (E_{bi}) from 1.2×10^7 V/m to 6.8×10^6 V/m for an ITO or sputtered ITO anode, respectively. Accumulated charge at the interface can result in an S-shaped J-V characteristic[16], which is not observed here. Therefore in calculating the electric field, we assume that all free carriers are depleted from the active region, and hence the field is uniform throughout the device. Without a sufficient E_{bi}, the charge separated pair that forms at the donor-acceptor interface on exciton dissociation is likely to recombine, leading

to reduced J_{SC} and V_{OC}. This is also reflected by the increase in the ideality factor from 1.89 ± 0.06 for the conventional cell, to 2.0 ± 0.1 for the inverted cell, indicating a larger recombination current. The decreased fill factor is primarily due to the higher series resistance of the device, a result of the higher contact resistance of the C_{60}/Al interface compared to that of an Al/C_{60} interface.

To increase V_{OC}, a series of inverted devices was fabricated with varied MoO_3 layer thicknesses (t) from 100 Å to 700 Å, while using a low work function, 5 vol. % Mg:Ag cathode. It was found that V_{OC} increases from 0.78 ± 0.02 V to 1.02 ± 0.02 V when t changes from 100 Å to 300 Å, and saturates for thicker MoO_3 films, as shown in Fig. 2a. Consistent with optical simulations, the responsivity peaks at t = 300 Å, yielding η_P =2.4 ± 0.2%, as shown in Fig. 2b.

The measured absorption of MoO_3 films on quartz substrates is shown in Fig. 3. The absorption edge corresponds to the MoO_3 band gap[17] (E_g). It is found to increase by 0.43 eV as t increases from 100 Å to 300 Å, and saturates thereafter. The absorption edge is also influenced by optical interference. After subtracting this effect, the increase in E_g is approximately 0.3 eV over this range of thicknesses. It has been found previously that the work function of MoO_3 (Φ_{MoO_3}) increases logarithmically with the layer thickness[18]. The energy shift improves device performance by: (1) creating a greater difference between the LUMO of MoO_3 and SubPc, thereby reducing the electron leakage current, and (2) promoting band bending in the highest occupied molecular orbitals (HOMO) of SubPc at the SubPc/MoO_3 interface.

The parallel resistance, R_P, and the photocurrent density, J_{ph}, are found at $J = 0$ using[19]:

$$V_{OC} = \frac{nkT}{q} \ln\left[\frac{J_{ph}(V_{OC})}{J_S} + 1 - \frac{V_{OC}}{R_P J_S}\right],$$

where q is the electron charge, k is the Boltzmann constant, and T is the absolute temperature. Typically[9] $J_{ph}/J_S >> 1$ and $V_{OC}/R_P << J_{ph}(V)$, and hence V_{OC} depends logarithmically on J_{ph}/J_S. By assuming a constant $J_{ph}(V) = J_{SC}$, the calculated V_{OC} matches the experimental data for conventional cells, but overestimates that of the inverted cells by 10% (see Table 1 and Fig. 2a, dashed line). This is likely due to the reduction in J_{ph} with increasing voltage, deviating from the assumption of a constant J_{ph}.

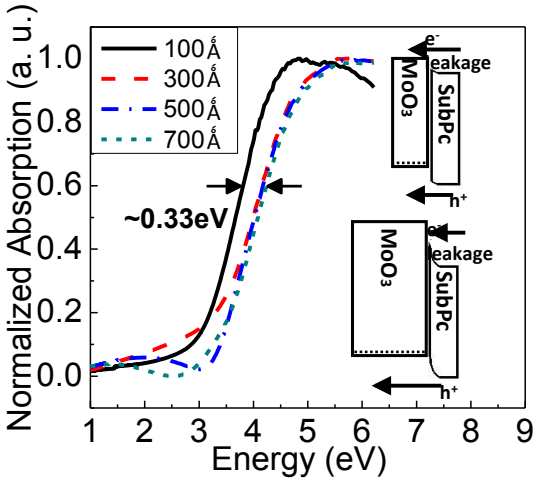

FIG. 3. (Color online) Measured absorption spectra for 100 Å (solid lines), 300 Å (dashed lines), 500 Å (dash-dotted lines), 700 Å (short dashed lines) thick MoO_3 films on quartz substrates. *Inset*: Schematic band diagram of the MoO_3/SubPc interface for a MoO_3 thickness of t =100 Å (upper) and 500 Å (lower).

As inferred from the energy level diagram of the MoO_3/SubPc interface in the inset of Fig. 3, the increase in Φ_{MoO_3} with thickness reduces the energy difference between the valence band maximum of MoO_3 and the HOMO of SubPc, consequently producing steeper band bending when these materials are brought into contact. This favors hole extraction from SubPc to the contact, reflected by the decrease in the ideality factor with MoO_3 thickness changing from 100 Å to 500 Å (see Table 1). When the MoO_3 thickness reaches 700 Å, however, the increase in device resistance becomes dominant and the ideality factor increases again. The combined effects of the reduced electron leakage and enhanced hole extraction due to the presence of MoO_3 results in a maximum V_{OC} = 1.02 ± 0.02 V, close to that of the conventional device.

Finally, the influence of the cathode work function (Φ_{Cat}) on performance was investigated, with results shown in Fig. 4. Values used for Φ_{Cat} are from Ref. 20. Here, 1000 Å

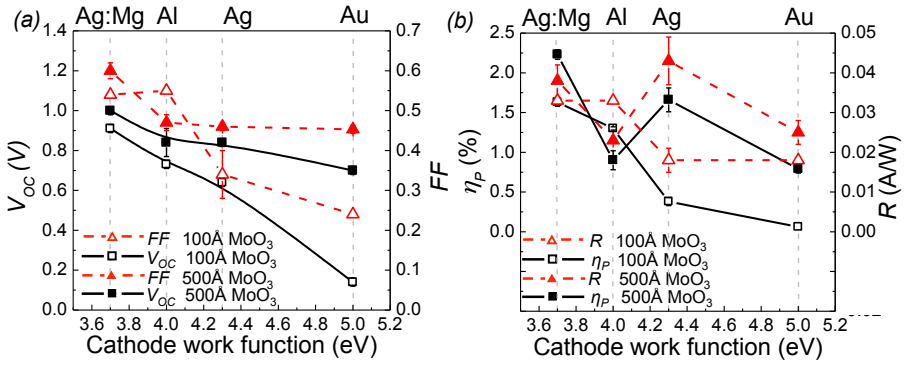

FIG. 4. (Color online) The influence of cathode work function (Φ_{Cat}) on device characteristics under 1 sun, AM1.5G illumination. Sample structure: glass/cathode 1000 Å/C_{60} 500 Å/SubPc 90 Å/MoO_3 t Å/ITO 400 Å with cathode compositions of Mg:Ag, Al, Ag, Au and t = 100 Å (open symbols) and 500 Å (closed symbols). Cathode work functions (from Ref. 20) are indicated by dashed vertical lines. *(a)* The dependence of *FF* (triangles and dashed lines) and V_{OC} (squares and solid lines) on Φ_{Cat}. *(b)* The dependence of η_p (squares and solid lines) and *R* (triangles and dashed lines) on Φ_{Cat}.

thick layers of Ag, Au, Al and Mg:Ag were used as cathodes, with MoO_3 t = 100 and 500 Å. For devices with t = 100 Å, V_{OC} increased significantly from 0.14 V to 0.91 V, while Φ_{Cat} decreased from 5.0 eV (Au) to 3.7 eV (Mg:Ag), as shown in Fig. 4a. Different cathode optical properties shift the optical field distribution, therefore changing the responsivity. The power conversion efficiency has a maximum at 2.23 ± 0.06% for Mg:Ag cathodes and t=500 Å MoO_3 (see Fig. 4b). The decrease in Φ_{Cat} results in an increased E_{bi} (from -1.9×10^7 V/m for Au to 1.2×10^7 V/m for Mg:Ag), leading to a higher V_{OC}. The built-in field for the Au-cathode devices is negative, giving rise to an increased electron leakage. Hence, the increase in t shows a much more dramatic impact on V_{OC} (from 0.91 V to 1.02 V for Mg:Ag and from 0.14 V to 0.7 V for Au). We conclude that to achieve a high-efficiency inverted cell, the electrodes must be chosen such that a sufficiently high E_{bi} is provided based on the energy levels of the photoactive layers and the contacts, and the electron leakage is effectively suppressed.

Note that there currently is disagreement as to the assignment of the energy levels of MoO_3. For example, there are reports that the conduction and valence band energies of MoO_3 are at E_C = 2.3eV and E_V = 5.2-5.3 eV[21, 22], while more recently, E_C = 6.7 eV and E_V = 9.7 eV[23]

have been reported. Since photoelectron spectroscopy used to measure these energies is sensitive to factors such as surface conditions and the presence of inter-gap defect states, variations in source materials and sample preparation conditions may lead to this discrepancy. Previously[9], where the growth conditions were nearly identical as in this work, MoO_3 was used as an electron blocking layer in organic solar cells with transport properties similar to those from an organic (SubPc) blocking layer where its HOMO energy is 5.6 eV and its LUMO is at 3.6 eV. Therefore, we conclude that it is likely that the MoO_3 film reported here has E_C = 2.3 eV and E_V = 5.3 eV, consistent with earlier reports. This assignment is consistent with measurements made in our laboratory, and to be reported elsewhere.

Table 1. Inverted solar cell performance for the structure: glass/Mg:Ag 1000 Å/C_{60} 500 Å/SubPc 90 Å/MoO_3 *t* Å/ITO 400 Å under simulated 1 sun, AM1.5G illumination.

***t* (Å)**	***R* (A/W)**	V_{OC} **(V)**	V_{OC} **(V) calculated**	η_p **(%)**	***n***	J_S **(mA/cm^2)**
100	0.030	0.78	0.87	1.21 ± 0.05	2.6 ± 0.06	7.6×10^{-6}
300	0.042	1.02	1.15	2.4 ± 0.2	2.4 ± 0.04	3.6×10^{-8}
500	0.038	1.00	1.15	2.23 ± 0.06	2.4 ± 0.01	3.6×10^{-8}
700	0.029	1.00	1.10	1.6 ± 0.1	2.7 ± 0.01	4.0×10^{-7}

In summary, 2.4 ± 0.2% power efficiency, inverted small molecule organic photovoltaic cells have been demonstrated for this program. We have shown that an organic cathode buffer layer is not necessary in either conventional or inverted planar SubPc/C_{60} OPVs. The inverted device performance can be substantially improved by employing a compound MoO_3/ITO anode that suppresses electron leakage while maximizing the incident optical field intensity in the

donor/acceptor interface region. The work function of layers adjacent to the donor or acceptor plays an important role in determining the V_{OC}.

References

1 P. Peumans, A. Yakimov, and S. R. Forrest, J. Appl. Phys. **93**, 3693-3723 (2003).

2 G. Parthasarathy, P. E. Burrows, V. Khalfin, V. G. Kozlov, and S. R. Forrest, Appl. Phys. Lett. **72**, 2138-2140 (1998).

3 J. Meiss, N. Allinger, M. K. Riede, and K. Leo, Appl. Phys. Lett. **93**, 103311-3 (2008).

4 J. Meiss, M. K. Riede, and K. Leo, J. Appl. Phys. **105**, 063108-5 (2009).

5 J. Meiss, M. K. Riede, and K. Leo, Appl. Phys. Lett. **94**, 013303-3 (2009).

6 X. Tong, R. F. Bailey-Salzman, G. Wei, and S. R. Forrest, Appl. Phys. Lett. **93**, 173304-3 (2008).

7 C. Tao, S. Ruan, X. Zhang, G. Xie, L. Shen, X. Kong, W. Dong, C. Liu, and W. Chen, Appl. Phys. Lett. **93**, 193307-3 (2008).

8 H. Schmidt, H. Flugge, T. Winkler, T. Bulow, T. Riedl, and W. Kowalsky, Appl. Phys. Lett. **94**, 243302-3 (2009).

9 N. Li, B. E. Lassiter, R. R. Lunt, G. Wei, and S. R. Forrest, Appl. Phys. Lett. **94**, 023307-3 (2009).

10 C. C. Wu, C. I. Wu, J. C. Sturm, and A. Kahn, Appl. Phys. Lett. **70**, 1348 (1997).

11 J. Xue and S. R. Forrest, J. Appl. Phys. **95**, 1869-1877 (2004).

12 V. Shrotriya, G. Li, Y. Yao, T. Moriarty, K. Emery, and Y. Yang, Advanced Functional Materials **16**, 2016-2023 (2006).

13 H. Gommans, B. Verreet, B. P. Rand, R. Muller, J. Poortmans, P. Heremans, and J. Genoe, Adv. Funct. Mater. **18**, 3686-3691 (2008).

14 C. Y. Kwong, A. B. Djurišić, and P. C. C. A. W. K. Chan, Jpn. J. Appl. Phys. **43**, 1305-1311 (2004).

15 J. Xue, S. Uchida, B. P. Rand, and S. R. Forrest, Appl. Phys. Lett. **84**, 3013-3015 (2004).

16 A. Kumar, S. Sista, and Y. Yang, J. Appl. Phys. **105**, 094512-6 (2009).

17 H. Y. Fan, Phys. Rev. **82**, 900 (1951).

18 Y. Kinoshita, R. Takenaka, and H. Murata, Appl. Phys. Lett. **92**, 243309-3 (2008).

19 B. P. Rand, D. P. Burk, and S. R. Forrest, Phys. Rev. B **75**, 115327-11 (2007).

20 M. A. Baldo and S. R. Forrest, Phys. Rev. B **64**, 085201 (2001).

21 F. Wang, X. Qiao, T. Xiong, and D. Ma, Organic Electronics **9**, 985-993 (2008).

22 V. Shrotriya, G. Li, Y. Yao, C. Chu, and Y. Yang, Appl. Phys. Lett. **88**, 073508-3 (2006).

23 M. Kroger, S. Hamwi, J. Meyer, T. Riedl, W. Kowalsky, and A. Kahn, Appl. Phys. Lett. **95**, 123301-3 (2009).